Comparison of the Beam Parameters corresponding to Corrugated Circular Waveguides and Planar Gratings

A. Jöstingmeier and M. Dohlus

Deutsches Elektronen-Synchrotron DESY
Gruppe Beschleunigerphysik
Notkestr. 85, D-22607 Hamburg, Germany

Abstract

The mode matching technique is used in order to calculate the electromagnetic field in a corrugated circular waveguide which is excited by an ultra-relativistic point charge moving along the longitudinal axis of the structure. It is shown how the standard representation of the beampipe field must be modified under these conditions. Some issues concerning the numerical implementation of the Bessel and Hankel functions are also discussed. The beam parameters of the structure which are the beam impedance, the wake function and the loss parameter per unit length are then derived. Numerical results are presented for various structures. They are compared with those of planar gratings which have recently been used as a model for the investigation of corrugated circular waveguides.

I. Introduction

The use of periodic structures as HOM (higher order modes) absorbers for TESLA was proposed in [1] and [2]. This initiated some investigations with the aim of computing the beam parameters of such structures [3], [4]. The proposed absorber looks like a corrugated circular waveguide which is schematically shown in Fig. 1(a). For the sake of simplicity, a planar grating which is presented in Fig. 1(b) was used as a model for the circular HOM absorber.

A similar model was also applied in order to estimate the longitudinal wakefield effects in the TESLA-TTF FEL undulator beampipe in [5]. If the surface structure is small compared to the radius of the beampipe and the wavelength of the electromagnetic field, then the surface can be described by an effective surface impedance. This quantity relates the components of the electric and the magnetic field which are tangential to the surface. Thus, this impedance is a property of the surface itself; and it does not depend on the geometry of the beampipe. On the other hand we have to keep in mind that the relation between the surface impedance and the beam parameters is in fact geometry dependent.

Another important application of the planar grating is that it may be used as a model in order to calculate the short range wake in constant impedance accelerating structures. This application is especially interesting for the FEL operation mode of TESLA [6] for which very short bunches are to be used.

For all three above mentioned applications of planar gratings as a model of circular structures it is important to find out what are the limitations of the planar model. The equivalence between corrugated circular waveguides and planar gratings was investigated in [3] in the following way: From [7] we know that the electromagnetic properties of a periodic structure and a dielectric layer are very similar as long as the wavelength is larger than the period length. In this frequency

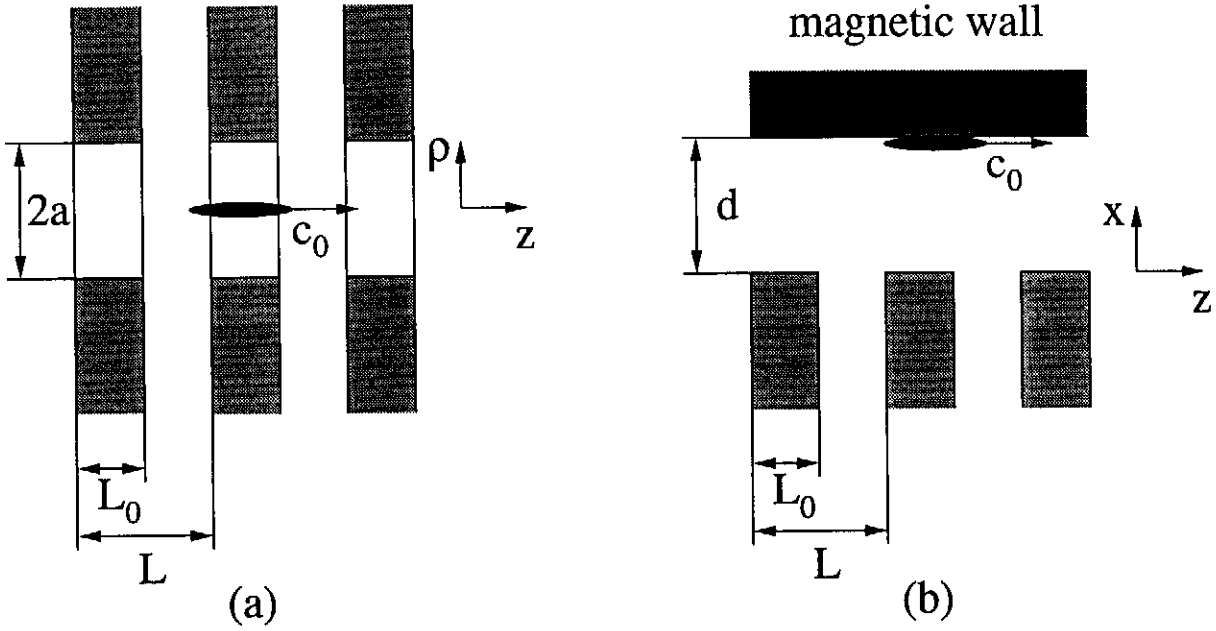

Figure 1: (a) Corrugated circular waveguide. (b) Planar grating.

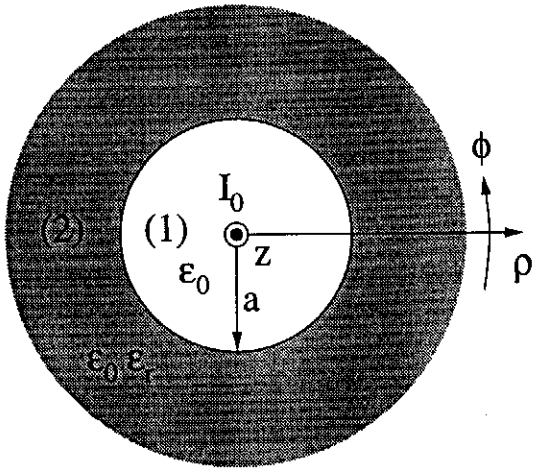

Figure 2: Circular two-layer problem.

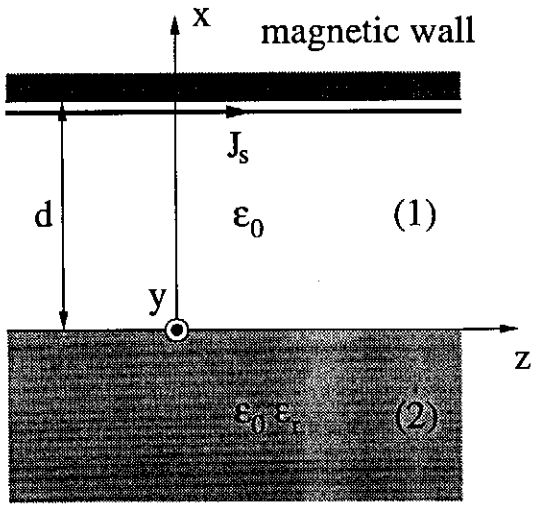

Figure 3: Planar two-layer problem.

range it is thus sufficient to demonstrate the equivalence between the two-layer problems which are shown in Figs. 2 and 3 in order to prove the equivalence between the originally periodic structures.

Analytic expressions for the beam impedances of the circular and the planar two-layer problem were derived in [3]. Note that the beam impedance of a periodic structure cannot be calculated such easy which is the reason why the two-layer problems were considered instead. These expressions were then compared in order to establish the conditions under which both structures are equivalent. It turned out that the beam impedance of a circular structure is just one half of that corresponding to a planar problem if we choose the distance between the magnetic wall and the dielectric layer as one half of the radius of the inner region of the circular

structure.

Note that the above statement concerning the equivalence of circular and planar two-layer problems is only valid if the frequency of the electromagnetic field is large enough so that asymptotic representations of the Hankel functions which describe the transverse field dependence may be used. This was also shown in [3]. We expect therefore that the beam impedance of a corrugated circular waveguide and the corresponding planar model are different for very low frequencies. This assumption is also confirmed by the numerical results which were presented in [3] and [8]: For the circular periodic structures, which were analyzed in [8], it was found that the beam impedance vanishes for the dc spectral line which is definitely not the case for the planar gratings which were examined in [3].

Very short bunches which excite wakefields with spectral components in the THz region where the wavelength is much shorter than the period length of the proposed HOM absorber will be used for the FEL operation mode of TESLA. At such high frequencies a periodic structure cannot be substituted by an equivalent two-layer problem. However, we excpect that a corrugated circular waveguide may be replaced by a planar grating especially in this frequency range where the free-space wavelength of the electromagnetic field is much shorter than the curvature of the beampipe. But we have to keep in mind that this assumption has not yet been proven.

In this contribution, the mode matching technique is therefore applied to calculate the electromagnetic field in a corrugated circular waveguide which is excited by an ultra-relativistic bunch of particles. The beam parameters of the structure which can be obtained from the field analysis are to be compared with those presented in [3] for a planar grating in order to find out under which conditions a planar model may be used for a circular structure.

II. Theory

This section is organized as follows: Subsection IIa) is dedicated to the calculation of the electromagnetic field in the circular structure by the application of the mode matching technique. Furthermore we compare the presented analysis with that of planar gratings. As a result of the field calculations we obtain the expansion coefficients of the spatial harmonics and the waveguides modes for a given frequency. In Subsection IIb) it is demonstrated how the beam parameters of the infinite periodic structure which are the beam impedance, the wake function and the loss parameter per unit length can be calculated from the field analysis of the previous subsection. The radial dependence of the electromagnetic field is described by Bessel and Hankel functions. Special problems concerning the numerical evaluation of these functions are discussed in Subsection IIc).

IIa) Field analysis

For the analysis of the corrugated cylindrical waveguide shown in Fig. 1(a) we use cylindrical coordinates ρ, ϕ and z. Nevertheless, it is convenient to write the current density $\boldsymbol{J}$ of the ultra-relativistic particle as a function of the corresponding transverse cartesian coordinates x and y:

$$\boldsymbol{J}(x,y,z,t) = q_0 c_0 \delta(x)\,\delta(y)\,\delta(z-c_0 t)\,\hat{\boldsymbol{e}}_z \quad , \tag{1}$$

where q_0, c_0, t and $\hat{\boldsymbol{e}}_z$ denote the charge of the particle, the intrinsic velocity of light, time and a unit vector in the axial direction, respectively. The Dirac delta-functions are normalized

according to

$$\int_{x=-\infty}^{\infty} \delta(x)\,dx = \int_{y=-\infty}^{\infty} \delta(y)\,dy = \int_{z=-\infty}^{\infty} \delta(z)\,dz = 1 \quad . \tag{2}$$

The Fourier transformation of $\boldsymbol{J}(x,y,z,t)$ is required for the application of the mode matching technique. Note that in this paper the Fourier transformation of a physical quantity is marked by a "~" in order to distinguish clearly between time and frequency domain. For $\tilde{\boldsymbol{J}}(x,y,z,\omega)$ we obtain straightforwardly

$$\tilde{\boldsymbol{J}}(x,y,z,\omega) = \int_{t=-\infty}^{\infty} \boldsymbol{J}(x,y,z,t)\,e^{-j\omega t}dt = q_0\delta(x)\,\delta(y)\,e^{-jk_0 z}\hat{\boldsymbol{e}}_z \quad , \tag{3}$$

where ω and k_0 are the angular frequency and the vacuum wavenumber of the electromagnetic field. Consequently, we get for the spectral representation of the beam current flowing along the z-axis

$$\tilde{I}(z,\omega) = \int_{x=-\infty}^{\infty}\int_{y=-\infty}^{\infty} \tilde{\boldsymbol{J}}(x,y,z,\omega)\cdot\hat{\boldsymbol{e}}_z dxdy = q_0 e^{-jk_0 z} \quad . \tag{4}$$

Due to the rotational symmetry of the structure only three components of the electromagnetic field are excited, namely, H_ϕ, E_ρ and E_z. Following the mode matching technique, we decompose the structure into two regions: (1) the beampipe region with $0 < \rho \le a$ and (2) the waveguide region with $a \le \rho < \infty$.

Let us start considering the electromagnetic field in region (1). It has been shown in [3] that the magnetic field in the beampipe region $\widetilde{H}_\phi^{(1)}$ satisfies the partial differential equation

$$\frac{\partial}{\partial\rho}\frac{1}{\rho}\frac{\partial\left(\rho\widetilde{H}_\phi^{(1)}\right)}{\partial\rho} + \frac{\partial^2\widetilde{H}_\phi^{(1)}}{\partial z^2} + k_0^2\widetilde{H}_\phi^{(1)} = 0 \quad . \tag{5}$$

$\widetilde{H}_\phi^{(1)}$ may be considered as a potential because the other components of the electromagnetic field can be derived from this quantity:

$$\tilde{E}_\rho^{(1)} = -\frac{Z_0}{jk_0}\frac{\partial\left(\widetilde{H}_\phi^{(1)}\right)}{\partial z} \quad , \tag{6}$$

$$\tilde{E}_z^{(1)} = \frac{Z_0}{jk_0}\frac{1}{\rho}\frac{\partial\left(\rho\widetilde{H}_\phi^{(1)}\right)}{\partial\rho} \quad , \tag{7}$$

where Z_0 denotes the intrinsic impedance of free-space.

The charged particle moves along the z-axis with c_0 and the electromagnetic field follows the particle with the same velocity. Consequently the phase advance of the field between two adjacent cells is just $-k_0 L$ where L is the period length. Thus the function $\widetilde{H}_\phi^{(1)}(\rho,z,\omega)\,e^{+jk_0 z}$ is periodic with respect to z:

$$\widetilde{H}_\phi^{(1)}(\rho,z+L,\omega)\,e^{+jk_0(z+L)} = \widetilde{H}_\phi^{(1)}(\rho,z,\omega)\,e^{+jk_0 z} \tag{8}$$

According to [9], $\widetilde{H}_\phi^{(1)}(\rho,z,\omega)$ can be represented as a superposition of an infinite number of spatial harmonics in the axial direction; whereas the radial field distribution is characterized by the first order Bessel function.

But one has to keep in mind that Eq. (5) degenerates to

$$\frac{\partial}{\partial\rho}\frac{1}{\rho}\frac{\partial\left(\rho\widetilde{H}_\phi^{(1)}\right)}{\partial\rho} = 0 \tag{9}$$

for $\partial/\partial z = -jk_0$. This case corresponds just to the zeroth order spatial harmonic which has thus to be treated separately. It is obvious that Eq. (9) is solved by

$$\widetilde{H}_\phi^{(1)} = \left(A\rho + \frac{B}{\rho}\right) e^{-jk_0 z} \quad , \tag{10}$$

where A and B are two still unknown integration constants. Hence the complete representation of the beampipe field reads

$$\widetilde{H}_\phi^{(1)}(\rho, z, \omega) = \sum_{\substack{m=-\infty \\ m\neq 0}}^{\infty} \mathcal{B}_m \mathrm{J}_1\left(k_{\rho m}^{(1)}\rho\right) e^{-j\alpha_m z} + \left(A\rho + \frac{B}{\rho}\right) e^{-jk_0 z} \quad , \tag{11}$$

$$\widetilde{E}_z^{(1)}(\rho, z, \omega) = \frac{Z_0}{jk_0}\left(\sum_{\substack{m=-\infty \\ m\neq 0}}^{\infty} \mathcal{B}_m k_{\rho m}^{(1)} \mathrm{J}_0\left(k_{\rho m}^{(1)}\rho\right) e^{-j\alpha_m z} + 2Ae^{-jk_0 z}\right) \quad , \tag{12}$$

where J_0 and J_1 are the Bessel functions of zeroth and first order [7]. The phase advance in the z-direction of the mth order spatial harmonic α_m is given by

$$\alpha_m = k_0 - m\frac{2\pi}{L} \quad . \tag{13}$$

The radial wavenumber $k_{\rho m}^{(1)}$ fulfills the separation condition

$$k_0^2 = {k_{\rho m}^{(1)}}^2 + \alpha_m^2 \tag{14}$$

and can therefore be calculated from the relation

$$k_{\rho m}^{(1)} = \begin{cases} \sqrt{k_0^2 - \alpha_n^2} & , \quad k_0 \geq \alpha_n \\ -j\sqrt{\alpha_n^2 - k_0^2} & , \quad k_0 < \alpha_n \end{cases} \quad . \tag{15}$$

Let us now compare the expansion of the beampipe field according to Eqs. (11) and (12) with that which has been used for the analysis of the equivalent planar problem in [3]. The latter field expansion is given by

$$\widetilde{H}_y^{(1)}(x, z, \omega) = \sum_{\substack{m=-\infty \\ m\neq 0}}^{\infty} \mathcal{B}_m \sin(\beta_m (d-x)) e^{-j\alpha_m z} + (A(d-x) + B) e^{-jk_0 z} \quad , \tag{16}$$

$$\widetilde{E}_z^{(1)}(x, z, \omega) = \frac{Z_0}{jk_0}\left(\sum_{\substack{m=-\infty \\ m\neq 0}}^{\infty} \mathcal{B}_m \beta_m \cos(\beta_m (d-x)) e^{-j\alpha_m z} + Ae^{-jk_0 z}\right) \quad . \tag{17}$$

The field components $\widetilde{H}_\phi^{(1)}(\rho, z, \omega)$ and $\widetilde{E}_z^{(1)}(\rho, z, \omega)$ of the circular structure are equivalent to $\widetilde{H}_y^{(1)}(x, z, \omega)$ and $\widetilde{E}_z^{(1)}(x, z, \omega)$ of the planar model. It is remarkable that both expansions are almost identical if one substitutes the phase advance in the x-direction β_m, the distance from the magnetic conducting wall $d - x$ and the trigonometric functions sin and cos by the corresponding quantities and functions of the circular structure, namely, $k_{\rho m}^{(1)}$, ρ, J_1 and J_0, respectively.

Only the zeroth order spatial harmonics are slightly different. If we consider the magnetic field, the second term of this harmonic reads B/ρ in the circular case, whereas we just have a

constant B for the planar grating. If we compare the expansions of the axial electric field, we find that the circular structure has an additional factor of 2 in front of the integration constant A which is typical.

Let us now proceed with the analysis of the corrugated circular waveguide. The integration constant B can be calculated immediately from the current flowing along the axis. Ampere's law says

$$\lim_{\rho\to 0} \oint_{C_\rho} \widetilde{H}_\phi^{(1)} \rho d\phi = \tilde{I} \quad . \tag{18}$$

If we insert Eqs. (4) and (11) into the above equation and keep in mind that $\lim_{z\to 0} \mathrm{J}_1(z) = 0$, it follows that

$$B = \frac{q_0}{2\pi} \quad . \tag{19}$$

The electromagnetic field in region (2) is expanded with respect to the complete set of eigenmodes of a circular parallel-plate waveguide [7]:

$$\widetilde{H}_\phi^{(2)} = \sum_{n=0}^{\infty} \mathcal{A}_n \cos(k_{zn} z)\, \mathrm{H}_1^{(2)}\left(k_{\rho n}^{(2)} \rho\right) \quad , \tag{20}$$

$$\widetilde{E}_z^{(2)} = Z_0 \sum_{n=0}^{\infty} \mathcal{A}_n \frac{k_{\rho n}^{(2)}}{jk_0} \cos(k_{zn} z)\, \mathrm{H}_0^{(2)}\left(k_{\rho n}^{(2)} \rho\right) \quad , \tag{21}$$

where $\mathrm{H}_0^{(2)}$ and $\mathrm{H}_1^{(2)}$ are the zeroth order and first order Hankel functions of second kind. These functions describe a radially outward propagating wave if the corresponding wavenumber $k_{\rho n}^{(2)}$ is real. The axial wavenumber k_{zn} is determined by the boundary conditions at $z = 0$ and $z = L_0$:

$$k_{zn} = \frac{n\pi}{L_0} \tag{22}$$

Note that the index n starts at $n = 0$ and that the corresponding eigenmode is TEM with respect to ρ. Making use of the separation condition

$$k_0^2 = {k_{\rho n}^{(2)}}^2 + k_{zn}^2 \quad , \tag{23}$$

we get for $k_{\rho n}^{(2)}$

$$k_{\rho n}^{(2)} = \begin{cases} \sqrt{k_0^2 - k_{zn}^2} & , \quad k_0 \geq k_{zn} \\ -j\sqrt{k_{zn}^2 - k_0^2} & , \quad k_0 < k_{zn} \end{cases} \quad . \tag{24}$$

In order to determine the unknown field expansion coefficients we exploit the continuity and boundary conditions of the axial electric and the azimuthal magnetic field at $\rho = a$. For the electric field we have

$$\widetilde{E}_z^{(1)}\Big|_{\rho=a} = \begin{cases} \widetilde{E}_z^{(2)}\Big|_{\rho=a} & , \quad 0 < z < L_0 \\ 0 & , \quad L_0 < z < L \end{cases} \quad . \tag{25}$$

Multiplying Eq. (25) by $e^{j\alpha_p z}$ and integrating both sides of the resulting equation over one period length yields the linear equations

$$\sum_{n=0}^{\infty} \frac{L_0}{L} \mathcal{A}_n k_{\rho n}^{(2)} \mathrm{H}_0^{(2)}\left(k_{\rho n}^{(2)} a\right) C_{pn} = \begin{cases} 2A & , \quad p = 0 \\ \mathcal{B}_p k_{\rho p}^{(1)} \mathrm{J}_0\left(k_{\rho p}^{(1)} a\right) & , \quad p = -\infty, \ldots, -1, +1, \ldots, +\infty \end{cases} \quad , \tag{26}$$

where the coupling integrals C_{pn} are exactly the same as those of the planar structure which has been investigated in [3]:

$$C_{pn} = \frac{1}{L_0} \int_{z=0}^{L_0} \cos(k_{zn} z)\, e^{j\alpha_p z} dz \quad . \tag{27}$$

The quantity C_{pn} describes the coupling between the pth spatial harmomic and the nth waveguide mode.

The continuity condition for the magnetic field reads

$$\widetilde{H}_{\phi}^{(1)}\Big|_{\rho=a} = \widetilde{H}_{\phi}^{(2)}\Big|_{\rho=a} \quad , \quad 0 \le z \le L_0 \quad . \tag{28}$$

If we multiply both sides of the above equation with $\cos(k_{zq} z)$ and integrate over the gap length L_0, we arrive at the linear system of equations

$$\mathcal{A}_q \frac{1+\delta_{0q}}{2} \mathrm{H}_1^{(2)}\left(k_{\rho q}^{(2)} a\right) = \sum_{\substack{m=-\infty \\ m\neq 0}}^{\infty} \mathcal{B}_m \mathrm{J}_1\left(k_{\rho m}^{(1)} a\right) C_{mq}^{*} + \left(Aa + \frac{q_0}{2\pi a}\right) C_{0q}^{*} \quad , \quad q = 0, \ldots, \infty \quad . \tag{29}$$

Let us define the following diagonal matrices for a concise notation of the final linear system of equations:

$$\left[\Lambda_{J_0}\right] = \mathrm{diag}\left\{\mathrm{J}_0\left(k_{\rho p}^{(1)} a\right)\right\} \quad , \quad p = -\infty, \ldots, -1, +1, \ldots, +\infty \tag{30}$$

$$\left[\Lambda_{J_1}\right] = \mathrm{diag}\left\{\mathrm{J}_1\left(k_{\rho p}^{(1)} a\right)\right\} \quad , \tag{31}$$

$$\left[\Lambda_{k_\rho^{(1)}}\right] = \mathrm{diag}\left\{k_{\rho p}^{(1)}\right\} \quad , \tag{32}$$

$$\left[\Lambda_{H_0^{(2)}}\right] = \mathrm{diag}\left\{\mathrm{H}_0\left(k_{\rho q}^{(2)} a\right)\right\} \quad , \quad q = 0, \ldots, \infty \tag{33}$$

$$\left[\Lambda_{H_1^{(2)}}\right] = \mathrm{diag}\left\{\mathrm{H}_1\left(k_{\rho q}^{(2)} a\right)\right\} \quad , \tag{34}$$

$$\left[\Lambda_{k_\rho^{(2)}}\right] = \mathrm{diag}\left\{k_{\rho q}^{(2)}\right\} \quad , \tag{35}$$

$$\left[\Lambda_N\right] = \mathrm{diag}\left\{\frac{1+\delta_{0q}}{2}\right\} \tag{36}$$

The coupling matrix $\left[C\right]$ is formed by the coupling integrals C_{pq}:

$$\left[C\right] = \{C_{pq}\} \quad , \quad p = -\infty, \ldots, -1, +1, \ldots, +\infty \quad , \quad q = 0, \ldots, \infty \tag{37}$$

Note that the zeroth order spatial harmonic is excluded from the coupling matrix. It is convenient that the coupling between this harmonic and the waveguide modes is taken into account by the column vector $\boldsymbol{V}$ which is defined as

$$\boldsymbol{V} = \begin{pmatrix} C_{00}^{*} \\ C_{01}^{*} \\ \vdots \\ C_{0q}^{*} \\ \vdots \end{pmatrix} \quad . \tag{38}$$

Moreover, let us define two further column vectors $\boldsymbol{\mathcal{A}}$ and $\boldsymbol{\mathcal{B}}$ which combine the field expansion coefficients of the waveguide modes and those of the spatial harmonics (except for that corresponding to the zeroth order spatial harmonic), respectively.

After eliminating A and $\boldsymbol{\mathcal{B}}$ from Eqs. (26) and (29), we finally obtain the linear system of equations

$$\left(\left[\Lambda_N\right]\left[\Lambda_{H_1^{(2)}}\right] - \frac{L_0}{L}\left[C\right]^{t*}\left[\Lambda_{J_1}\right]\left[\Lambda_{k_\rho^{(1)}}\right]^{-1}\left[\Lambda_{J_0}\right]^{-1}\left[C\right]\left[\Lambda_{k_\rho^{(2)}}\right]\left[\Lambda_{H_0^{(2)}}\right] - \frac{a}{2}\frac{L_0}{L}\boldsymbol{V}\boldsymbol{V}^{t*}\left[\Lambda_{k_\rho^{(2)}}\right]\left[\Lambda_{H_0^{(2)}}\right]\right)\boldsymbol{\mathcal{A}} = \frac{q_0}{2\pi a}\boldsymbol{V} \tag{39}$$

which determines $\boldsymbol{\mathcal{A}}$. These equations are usually denoted as the characteristic system of equations of a field problem. The other field expansion coefficients can then be calculated from

$$\boldsymbol{\mathcal{B}} = \frac{L_0}{L}\left[\Lambda_{k_\rho^{(1)}}\right]^{-1}\left[\Lambda_{J_0}\right]^{-1}\left[C\right]\left[\Lambda_{k_\rho^{(2)}}\right]\left[\Lambda_{H_0^{(2)}}\right]\boldsymbol{\mathcal{A}} \quad , \tag{40}$$

$$A = \frac{1}{2}\frac{L_0}{L}\boldsymbol{V}^{t*}\left[\Lambda_{k_\rho^{(2)}}\right]\left[\Lambda_{H_0^{(2)}}\right]\boldsymbol{\mathcal{A}} \quad . \tag{41}$$

IIb) Beam parameters

The beam impedance per unit length of an infinite periodic structure $Z'(k_0)$ is defined as the Fourier transformation of the delta-wake per unit length $W^{\delta\prime}(s)$:

$$Z'(k_0) = \frac{1}{c_0}\int_{s=-\infty}^{\infty} W^{\delta\prime}(s)\, e^{-jk_0 s} ds \tag{42}$$

$W^{\delta\prime}(s)$ can be calculated from the limit

$$W^{\delta\prime}(s) = \frac{1}{q_0}\lim_{z\to\infty}\frac{1}{2z}\int_{\xi=-z}^{z} E_z^{(1)}\left(\rho = 0, \xi, t = \frac{s+\xi}{c_0}\right) d\xi \quad . \tag{43}$$

Inserting the representation of the electric field in the beampipe region according to Eq. (12) into the above equation, yields

$$\frac{Z'(k_0)}{Z_0/L} = \frac{2}{jk_0 L}\frac{A}{q_0/L^2} \quad . \tag{44}$$

Note that the term $A/(q_0/L^2)$ is the normalized expansion coefficient of the zeroth order spatial harmonic as it comes out of the computer. Thus the above equation means that the beam impedance per unit length is basically given by this expansion coefficient divided by the wavenumber.

Following the analysis which has been presented in [3] for a planar grating, we obtain for the wake and the loss parameter per unit length $W'(s)$ and k', respectively,

$$W'(s) = \frac{c_0}{2\pi}\int_{k_0=-\infty}^{\infty} Z'(k_0)\,\tilde{\lambda}(k_0)\, e^{jk_0 s} dk_0 \quad , \tag{45}$$

$$k' = -\frac{c_0}{2\pi}\int_{k_0=-\infty}^{\infty} Z'(k_0)\left|\tilde{\lambda}(k_0)\right|^2 dk_0 \quad , \tag{46}$$

where $\tilde{\lambda}(k_0)$ denotes the bunch spectrum. For a Gaussian bunch the spectrum reads

$$\tilde{\lambda}(k_0) = e^{-\frac{1}{2}(k_0\sigma)^2} \quad , \tag{47}$$

where σ is the rms bunch length.

(48)

IIc) Special functions

The functions describing the radial dependence of the electromagnetic field in the beampipe (waveguide) region are the Bessel (Hankel) functions. When $k_{\rho m}^{(1)^2}$ $\left(k_{\rho n}^{(2)^2}\right)$ is negative, $k_{\rho m}^{(1)}$ $\left(k_{\rho n}^{(2)}\right)$ is pure imaginary. If we let $k_{\rho m}^{(1)} = -j\left|k_{\rho m}^{(1)}\right|$ $\left(k_{\rho n}^{(2)} = -j\left|k_{\rho n}^{(2)}\right|\right)$, the solutions are given by $\mathrm{J}_\nu\left(-j\left|k_{\rho m}^{(1)}\right|\rho\right)$ $\left(\mathrm{H}_\nu^{(2)}\left(-j\left|k_{\rho n}^{(2)}\right|\rho\right)\right)$. It is possible to substitute these functions of a pure imaginary argument by the modified Bessel functions I_ν (K_ν) of a real argument:

$$\mathrm{I}_\nu(y) = j^\nu \mathrm{J}_\nu(-jy) \quad , \tag{49}$$

$$\mathrm{K}_\nu(y) = \frac{\pi}{2}(j)^{\nu+1}\,\mathrm{H}_\nu^{(2)}(-jy) \tag{50}$$

However, we do not make use of the modified Bessel functions. We rather consider the $\mathrm{J}_\nu\left(k_{\rho m}^{(1)}\rho\right)$ $\left(\mathrm{H}_\nu^{(2)}\left(k_{\rho n}^{(2)}\rho\right)\right)$ as functions of a complex argument as they are provided bei the NAG library in order to keep our source code simple.

From the asymptotic behaviour of the modified functions I_ν (K_ν) which is

$$\mathrm{I}_\nu(y) \propto \frac{e^y}{\sqrt{y}} \quad \text{for} \quad y \to \infty \quad , \tag{51}$$

$$\mathrm{K}_\nu(y) \propto \frac{e^{-y}}{\sqrt{y}} \tag{52}$$

it can be concluded that the values $\mathrm{J}_\nu\left(k_{\rho m}^{(1)}a\right)$ $\left(\mathrm{H}_\nu^{(2)}\left(k_{\rho n}^{(2)}a\right)\right)$ become very large (small) for higher order spatial harmonics (for waveguide modes with a high axial order). Thus scaled versions of these functions have to be used in order to avoid a numerical overflow (underflow). The corresponding scaled values $\bar{\mathrm{J}}_\nu$ $\left(\bar{\mathrm{H}}_\nu^{(2)}\right)$ are defined by

$$\mathrm{J}_\nu(-j\,|y|) = \bar{\mathrm{J}}_\nu(-j\,|y|)\,e^{|y|} \quad , \tag{53}$$

$$\mathrm{H}_\nu^{(2)}(-j\,|y|) = \bar{\mathrm{H}}_\nu^{(2)}(-j\,|y|)\,e^{-|y|} \quad . \tag{54}$$

These scaled values can also be calculated using the NAG library.

III. Numerical results

In Subsection IIIa) we check the continuity of the field components H_ϕ and E_z at $\rho = a$ in order to prove the validity of the presented method. Furthermore a detailed study of convergence is also carried out in this subsection. In Subsection IIIb) we compare the beam parameters of circular structures with those of the corresponding planar gratings for an excitation with short and long Gaussian bunches. From this comparison we can conclude under which conditions we may use the planar structure as a model for the circular one.

IIIa) Corrugated circular waveguides

In order to check the validity of the developed analysis let us compare the beampipe and the waveguide field at $\rho = a$. Figs. 4 and 5 show the corresponding real part of the axial electric

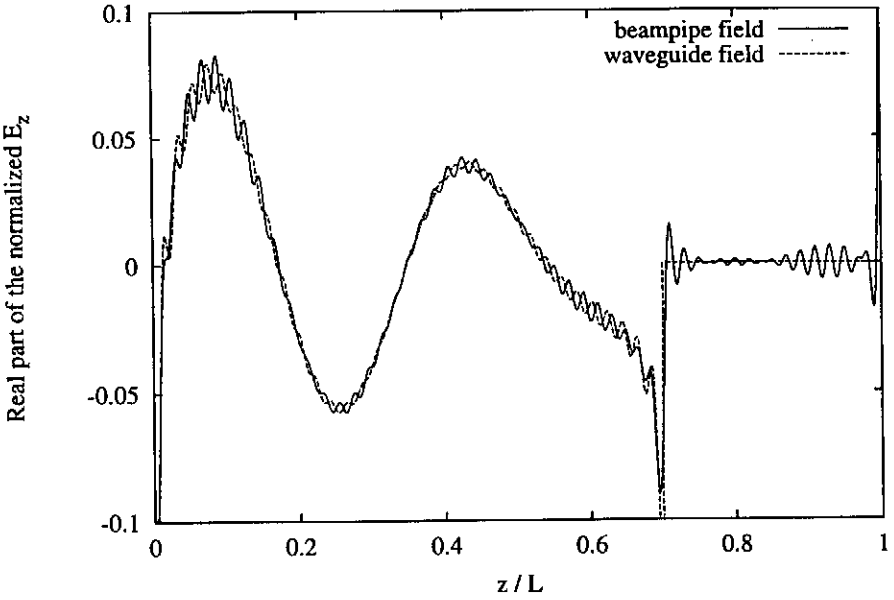

Figure 4: Real part of the normalized axial electric field along $\rho = a$. Parameters: $L_0 = 0.7L$, $a = 0.5L$ and $k_0 L = 20$.

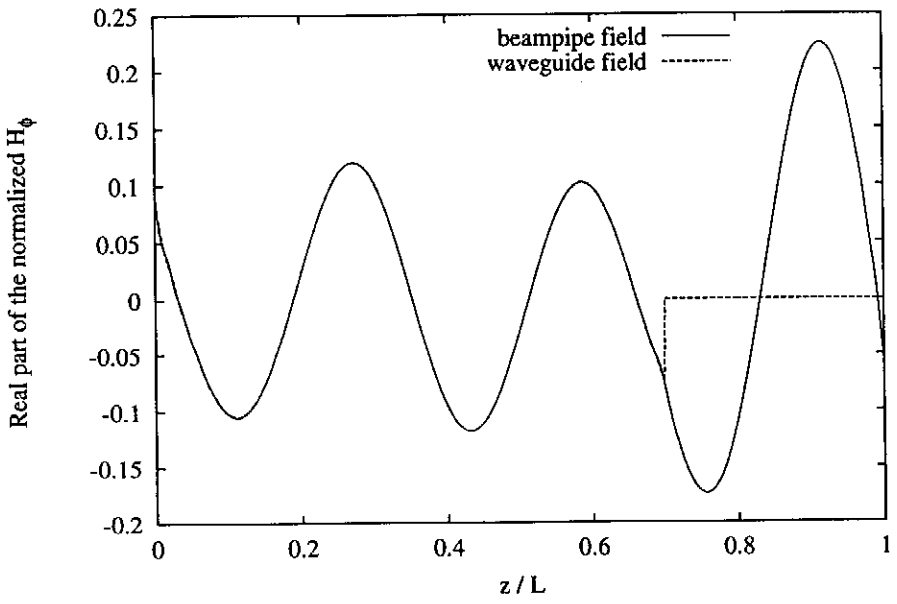

Figure 5: Real part of the normalized azimuthal magnetic field along $\rho = a$. Parameters: see Fig. 4.

and the azimuthal magnetic field. The parameters of the investigated structure are $L_0 = 0.7L$, $a = 0.5L$ and $k_0 L = 20$. This wavenumber means that the frequency of the electromagnetic field is about 100 Ghz if we assume a period length of 10 cm.

The axial electric field shows the well-known singularities at $z = 0$ and $z = L_0$ due to the 90°-edges at these locations [10]. This phenomenon leads to relative strong oscillations of the field distributions. Nevertheless, the agreement between the beampipe and the waveguide field is quite good for $0 < z < L_0$. On the other hand, for $L_0 < z < L$, the waveguide field is not defined and the beampipe field must vanish as it is the case.

The azimuthal magnetic field is parallel to the edges. This field component is consequently well-behaved everywhere. The corresponding curves for the beampipe and the waveguide field, which are presented in Fig. 5, are very smooth and agree almost perfectly within $0 \leq z \leq L_0$.

An infinite number of spatial harmonics and waveguide modes has been used for the representation of the electromagnetic field in the beampipe and the waveguide region. However, these series have to be truncated for the practical evaluation of the mode matching technique. The results presented in Figs. 4 and 5 have been calculated using the relatively large number of 50 spatial harmonics and a correspondingly high number of waveguide modes. But one has to keep in mind that the number of field expansion terms should not be chosen much higher than necessary in order to keep the presented method numerically efficient. This is due to the fact that the size of the characteristic system of equations linearly increases with the number of field expansion terms. A systematic study of the convergence of the results with respect to the number of these terms is therefore required.

Fig. 6 shows the real part of the normalized beam impedance per unit length as a function of the number of spatial harmonics with the free-space wavenumber of the electromagnetic field as a parameter. From this figure it can be concluded that the number of field expansion terms has to be approximately linearly increased with the frequency of the electromagnetic field. According to Fig. 6, the minimum number of spatial harmonics which must be taken into account in order to get stable results is 7, 16 and 32 for a normalized wavenumber $k_0 L$ of 20, 50 and 100, respectively.

Figs. 7 and 8 present the real part of the beam impedance per unit length as a function of the free-space wavenumber of the electromagnetic field with the number of spatial harmonics as a parameter. From Fig. 6 it can be predicted that the curves which have been calculated with $N_{har} = 50$ are accurate at least until $k_0 L = 150$ which is twice the maximum frequency that is considered in Figs. 7 and 8. Thus the curves with $N_{har} = 50$ may serve as reference results.

It can be concluded from Fig. 6 by interpolation that the computation of the beam impedance using 10 spatial harmonics should be accurate up to a maximum wavenumber of about 30. This estimation is indeed confirmed by Fig. 7 in which the two presented curves start to deviate at $k_0 L \approx 32$. It is remarkable that the loss of accuracy occurs quite suddenly. This phenomenon is also observed in Fig. 8. In this figure it is furthermore demonstrated that the wavenumber up to which we get accurate results can be doubled if we use 20 spatial harmonics instead of 10.

IIIb) Comparison between corrugated circular waveguides and planar gratings

Let us now compare the beam parameters of a corrugated circular waveguide with those of a planar grating. Fig. 9 shows the real part of the normalized beam impedances per unit length

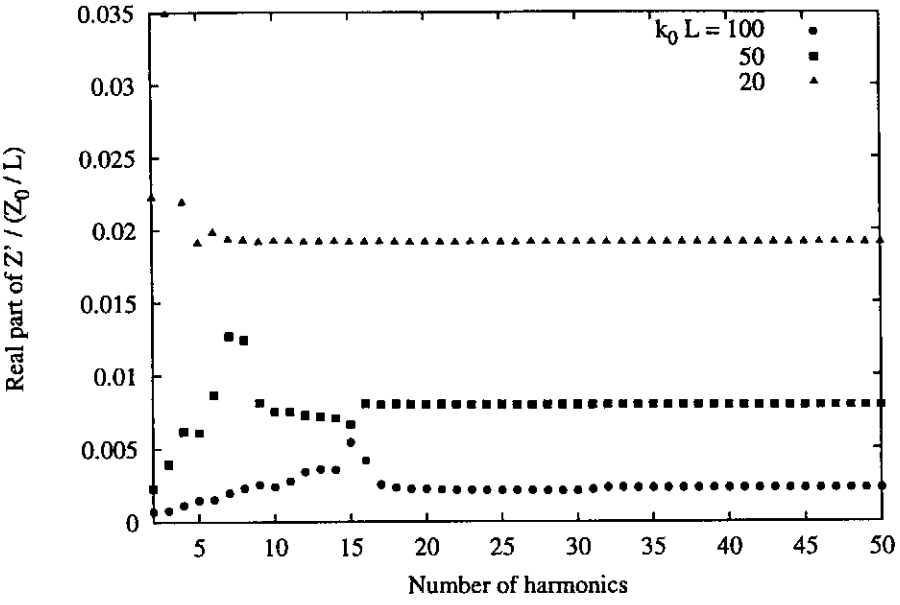

Figure 6: Real part of the normalized beam impedance per unit length as a function of the number of spatial harmonics with the free-space wavenumber of the electromagnetic field as a parameter. Parameters: see Fig. 4.

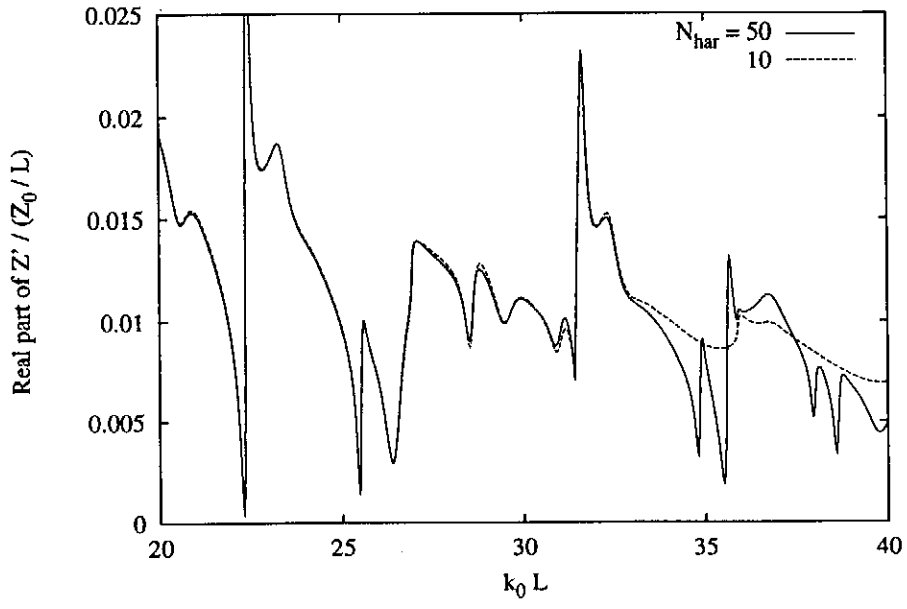

Figure 7: Real part of the normalized beam impedance per unit length as a function of the free-space wavenumber of the electromagnetic field with the number of spatial harmonics as a parameter. Parameters: see Fig. 4.

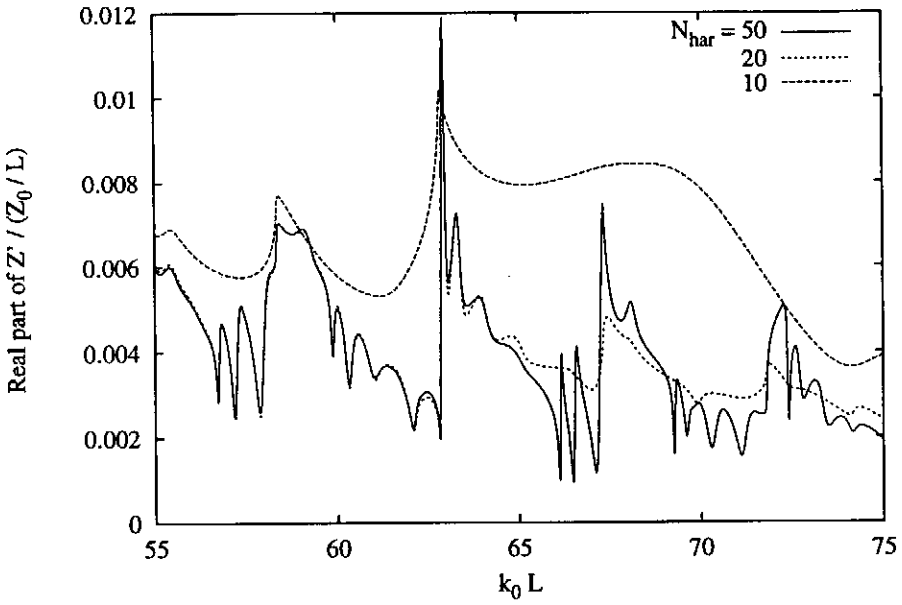

Figure 8: Real part of the normalized beam impedance per unit length as a function of the free-space wavenumber of the electromagnetic field with the number of spatial harmonics as a parameter. Parameters: see Fig. 4.

for both configurations. The radius of the beampipe is assumed to be much larger than the period length ($a/L = 20$) as it is also the case for the proposed TESLA absorber.

It is noticeable that in the considered frequency range the characteristic of the curves changes significantly at $k_0 L = \pi$ and $k_0 L = \pi/(L_0/L)$. This can be explained by the fact that at this wavenumbers the first higher order spatial harmonic and the first higher order waveguide mode turn from evanescent to propagating in the radial direction. On the other hand, all higher order modes are evanescent below $k_0 L = \pi$ so that the frequency characteristic of the beam impedance is very smooth in this frequency range.

The agreement between both curves is quite good except for very small wavenumbers. This is illustrated in more detail in Fig. 10 from which it can clearly be seen that the beam impedance of a circular structure linearly tends to zero at $k_0 L = 0$; whereas the beam impedance of a planar structure approaches a constant for $k_0 L \to 0$.

Let us now examine what is the effect of this disagreement of the beam impedances at low frequencies on the wake function. Fig. 11 shows the normalized wake per unit length of both types of structures for a relatively long Gaussian bunch with an rms length of $10L$. The normalized bunch shape is also given in this figure.

The two wake functions which are presented in Fig. 11 can clearly be distinguished. The maximum of the wake per unit length corresponding to the planar structure is about 15% higher than that corresponding to the corrugated circular waveguide. Furthermore, the wake function of the planar structure is positive for all s; whereas we have $\int_{s=-\infty}^{\infty} W'(s)\, ds = 0$ for the circular configuration.

From Eq. (45) it follows that the wake function per unit length is the inverse Fourier transformation of the beam impedance per unit length times the bunch spectrum. The wake function is therefore basically determined by the low frequency part of the spectral distribution of the beam impedance if we excite a structure by a long bunch, which has a narrow spectral width,

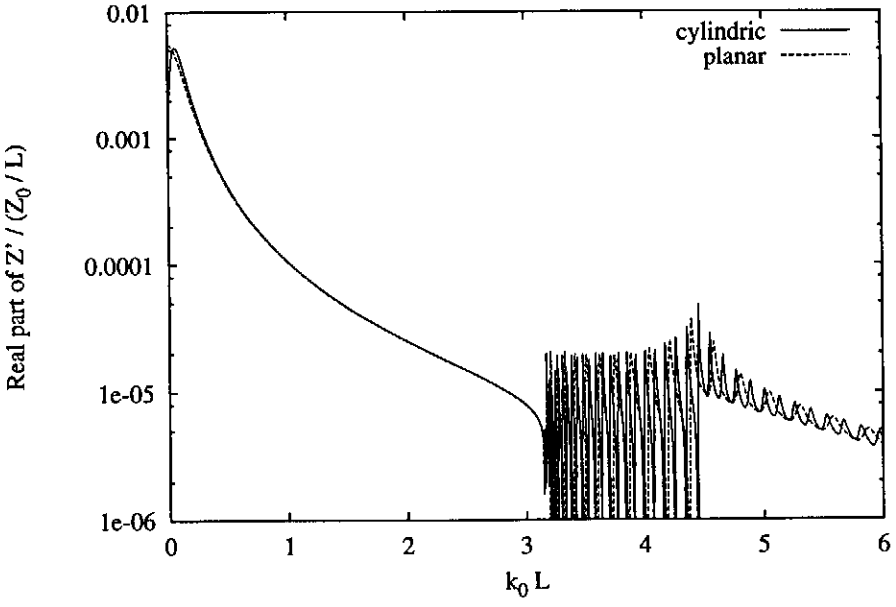

Figure 9: Comparison between the real part of the normalized beam impedance per unit length corresponding to a corrugated circular waveguide and a planar grating over a broad range of wavenumbers. Parameters: $L_0 = 0.7L$, $a = 20L$.

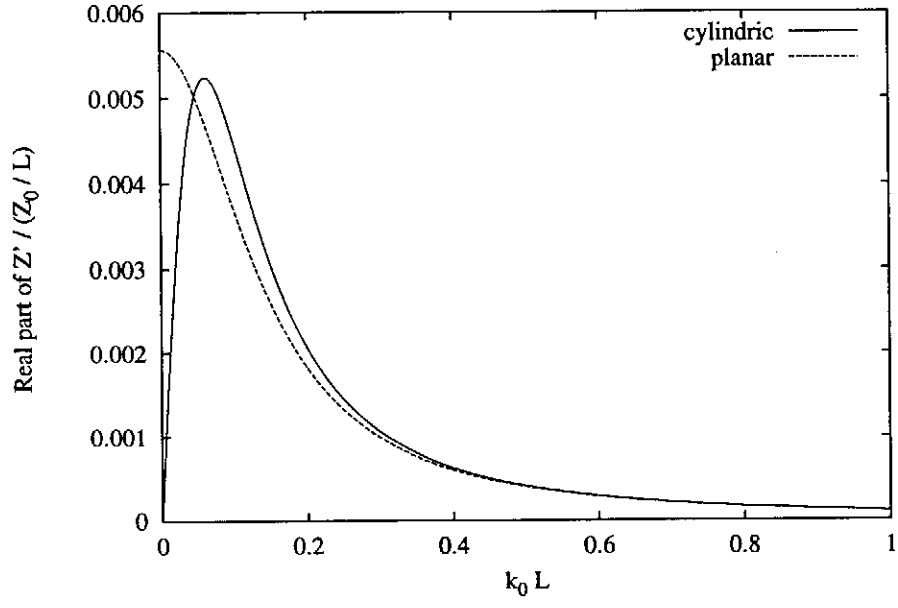

Figure 10: Comparison between the real part of the normalized beam impedance per unit length corresponding to a corrugated circular waveguide and a planar grating for small wavenumbers. Parameters: see Fig. 9.

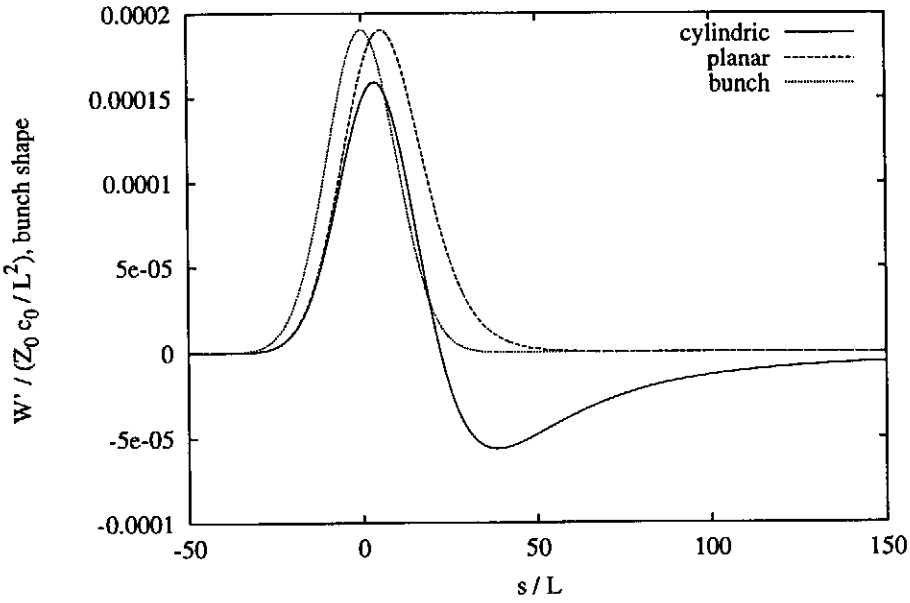

Figure 11: Comparison between the normalized wake per unit length corresponding to a corrugated circular waveguide and a planar grating for a bunch which is long compared to the period length of the periodic structure. Parameters: see Fig. 9 and $\sigma = 10L$.

as it is the case in Fig. 11. According to Fig. 10, the beam impedances of the circular and the planar configuration are quite different for small wavenumbers. Hence it is obvious that the agreement between the wake functions is poor if the structures are excited by such a bunch. Moreover, the phenomenon that the net area under the wake function for the circular structure vanishes can be explained by the fact that the dc spectral component of the corresponding beam impedance also vanishes.

If a structure is excited by a short bunch of particles the short range wake is mainly given by the frequency dependence of the beam impedance per unit length for large wavenumbers. Fig. 12 shows the comparison between the normalized short range wake per unit length corresponding to a corrugated circular waveguide and a planar grating for a bunch with a rms length of $0.2L$. The agreement of both wake functions is excellent in the range from $-5\sigma \leq s \leq +5\sigma$. However, if we consider the corresponding long range wake, which is presented in Fig. 13, the same characteristic differences between both wake functions which already have been found out in Fig. 11 are observed again.

Fig. 14 shows the normalized loss parameters per unit length as a function of the rms bunch length for a corrugated circular waveguide and the corresponding planar model. It turns that the planar model yields accurate results as long as the bunch length is short compared to the period length which is expected from the previous investigations concerning the calculation of wake functions.

IV. Conclusions

The mode matching technique has been employed for the computation of the beam parameters of a corrugated circular waveguide which is excited by an ultra-relativistic bunch travelling in

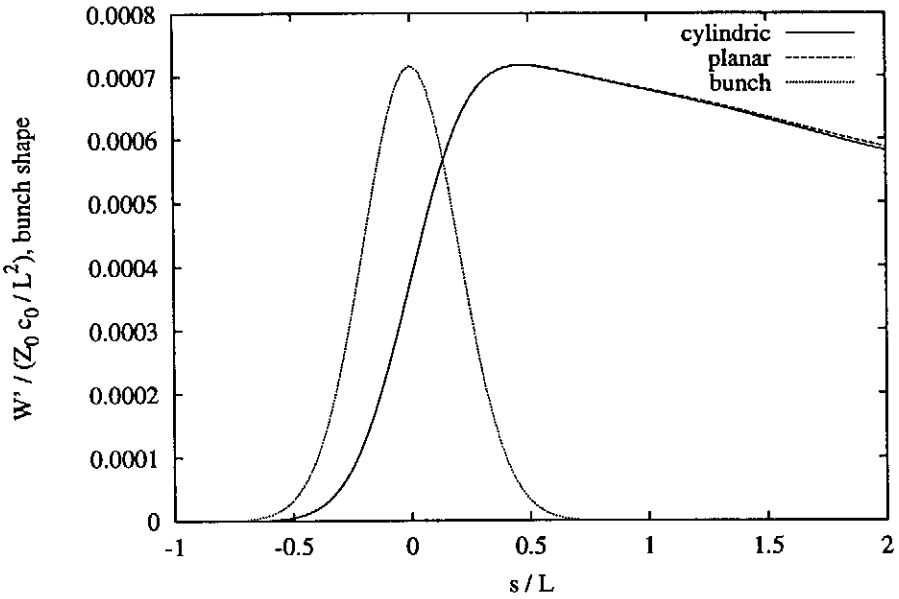

Figure 12: Comparison between the normalized short range wake per unit length corresponding to a corrugated circular waveguide and a planar grating for a bunch which is short compared to the period length of the periodic structure. Parameters: see Fig. 9 and $\sigma = 0.2L$.

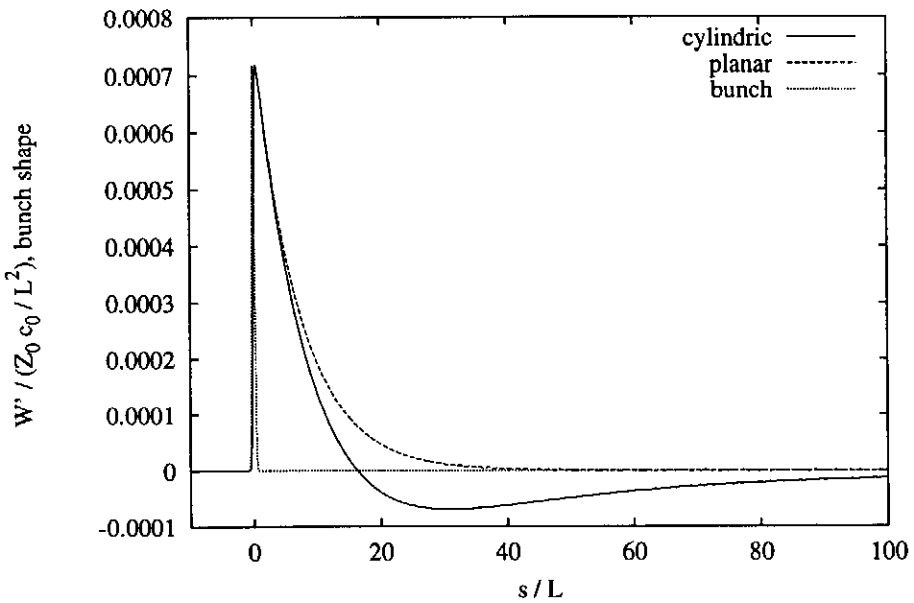

Figure 13: Comparison between the normalized long range wake per unit length corresponding to a corrugated circular waveguide and a planar grating for a bunch which is short compared to the period length of the periodic structure. Parameters: see Fig. 12.

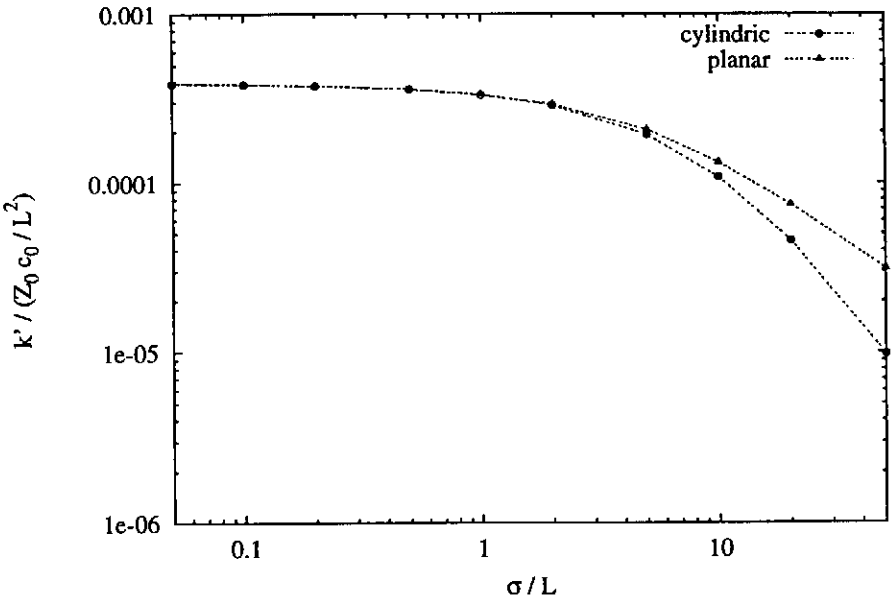

Figure 14: Comparison between the normalized loss parameter per unit length corresponding to a corrugated circular waveguide and a planar grating. Parameters: see Fig. 9

the axial direction of the structure. The numerical results of this analysis have been compared with those corresponding to planar gratings which have served as a model for circular structures in previous investigations. It has turned out that the beam impedance corresponding to the two kinds of structures is very similar except for very low frequencies. The dc spectral component of the beam impedance of circular structures vanishes; whereas this is not the case for planar gratings. Moreover it has been found out that for long bunches the wake function and the loss parameter of circular waveguides are quite different from those which have been calculated for planar gratings. But the numerical investigations show also that if one is basically interested in the short range wake for short bunches one may use the planar grating model even if accurate results are required.

Acknowledgement

The authors are indebted to many colleagues from the TESLA collaboration who contributed to these ideas.

References

[1] M. Dohlus, N. Holtkamp and A. Jöstingmeier, "Design of a broadband absorber for $f >$ 100 GHz", *Meeting note: 26 Linear collider project meeting at DESY*, 1997.

[2] M. Dohlus, N. Holtkamp, A. Jöstingmeier, H. Hartwig and D. Trines, "Design of a HOM broadband absorber for TESLA", *Meeting note: 31 Linear collider project meeting at DESY*, 1998.

[3] A. Jöstingmeier, M. Dohlus and N. Holtkamp, "Application of the mode matching technique for the computation of the beam parameters of an infinite periodic structure", DESY, TESLA 98-23, 1998.

[4] A. Jöstingmeier, M. Dohlus and N. Holtkamp, "Computation of the absorption characteristics of a two-dimensional rectangular waveguide array using the mode matching technique", DESY, TESLA 98-23, 1998.

[5] M. Dohlus, R. Lorenz, T. Kamps, H. Schlarp and R. Wanzenberg, "Estimation of longitudinal wakefield effects in the TESLA-TTF FEL undulator beam pipe and diagnostic section", DESY, TESLA 98-02, 1998.

[6] R. Brinkmann *et al.* (ed.), *Conceptual design of a 500 GeV e^+e^- linear collider with integrated X-ray laser facility*, DESY 1997-048, 1997.

[7] H.-G. Unger, *Elektromagnetische Theorie für die Hochfrequenztechnik*, Hüthig, 1981.

[8] H. Henke, "Point charge passing a resonator with beam tubes", *Archiv für Elektrotechnik*, vol. 69, pp. 271–277, 1986.

[9] D. Maystre, "Rigorous vector theories of diffraction gratings", *Progress in Optics*, vol. 21, Elsevier Sci. Pub., pp. 1–70, 1984

[10] R. E. Collin, *Field Theory of Guided Waves*, IEEE PRESS, 1991.